SUPPORTING INFORMATION

TITLE: Orientation of Ligand Field for Dangling Manganese in Photosynthetic Oxygen-Evolving Complex of Photosystem II

AUTHORS: Hiroyuki Mino* and Hiroki Nagashima‡

Division of Material Science, Graduate School of Science, Nagoya University, Furo-cho, Chikusa-ku, 464-8602, Nagoya, Aichi, Japan.

Present Addresses
‡Hiroki Nagashima, Department of Chemistry, Graduate School of Science and Engineering, Saitama University, 255 Shimo-Okubo, Sakura-ku, Saitama 338-8570, Japan

The supporting information containing Figure S1-S8

Corresponding Author
***Hiroyuki Mino, Tel: +81-52-789-2882; Email: mino@bio.phys.nagoya-u.ac.jp**

CONTENTS

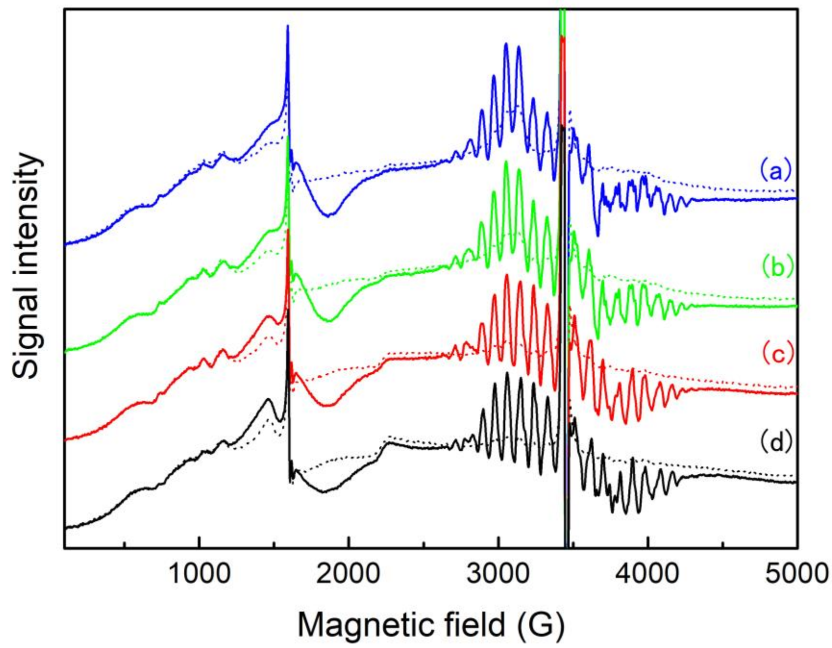

Figure S1. EPR spectra of the oriented PS II membranes in (solid line) S_2 state (dotted line) S_1 state measured at the angle of (a) 0°, (b) 30°, (c) 60°, and (d) 90° of the external magnetic field $\boldsymbol{B_0}$ relative to the membrane normal $\boldsymbol{n}$. Experimental conditions: microwave frequency, 9.67 GHz; microwave power, 4 mW; modulation frequency, 100 kHz; modulation amplitude, 10 G.

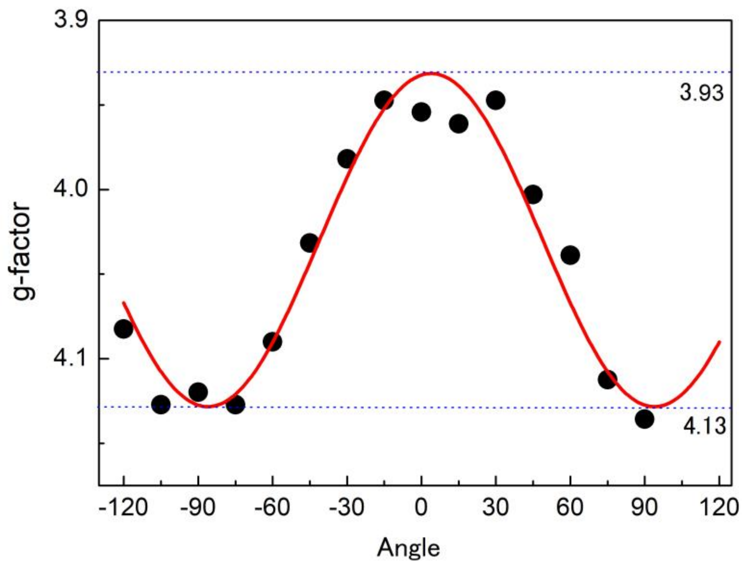

Figure S2. The orientation dependence of the *g*-values, converted from the resonant fields of the g = 4.1 signal relative to the angle between the external magnetic field $\boldsymbol{B_0}$ and the membrane normal $\boldsymbol{n}$. The orientation dependence was fitted by a sine function (solid line). The dotted lines show the maximum and minimum *g*-values. Experimental conditions are the same as fig. S1.

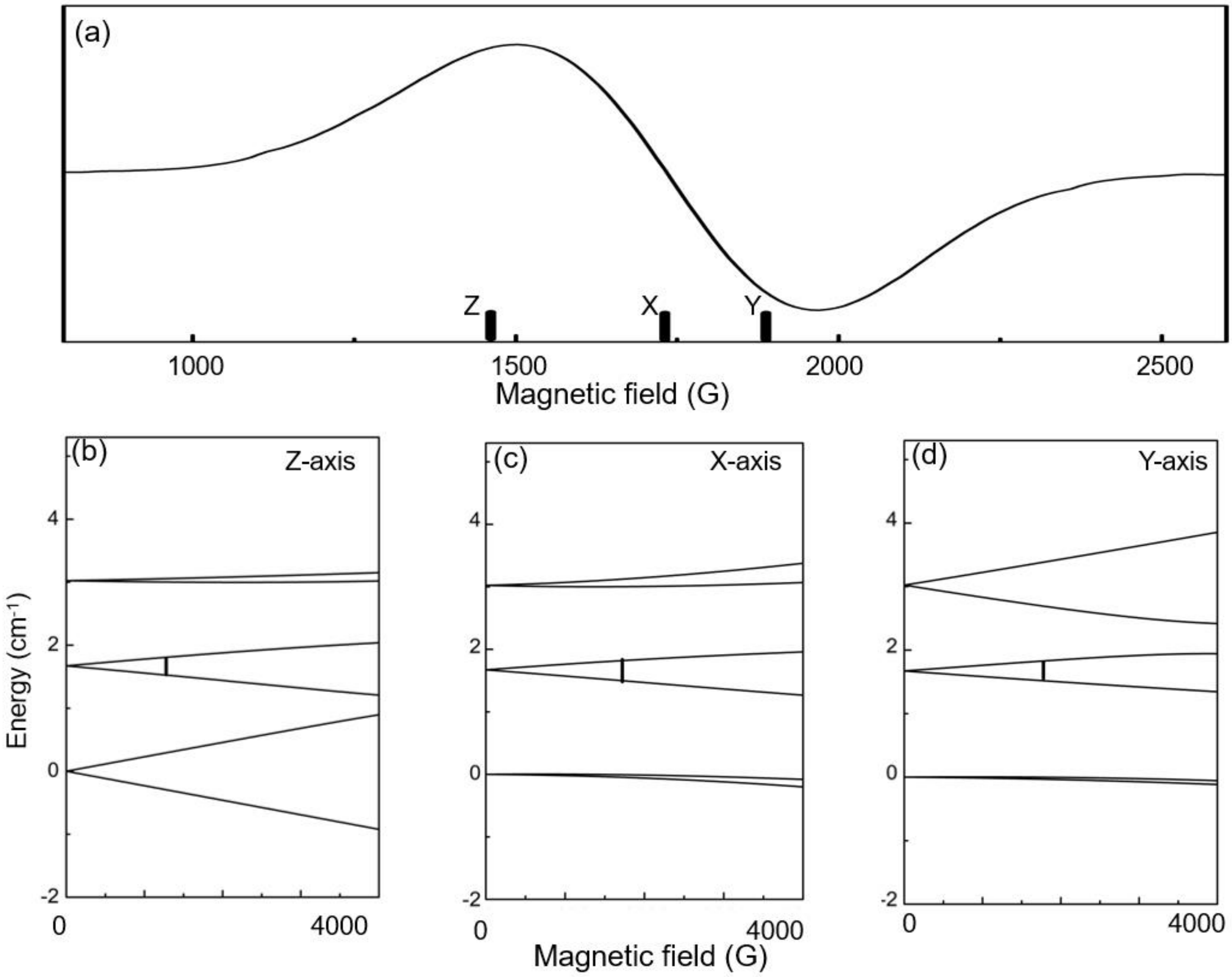

Figure S3. (a) The powder pattern of the EPR spectrum for the g = 4.1 signal using the single-spin model. (b-d) The energy block diagrams, where the external field $\boldsymbol{B_0}$ is directed along (b) D_Z-axis, (c) D_X-axis and (d) D_Y-axis. The parameters: microwave frequency, 9.67 GHz; g = 2; $\boldsymbol{S}$ = 5/2; D = -0.455 cm^{-1}; E/D = 0.25.

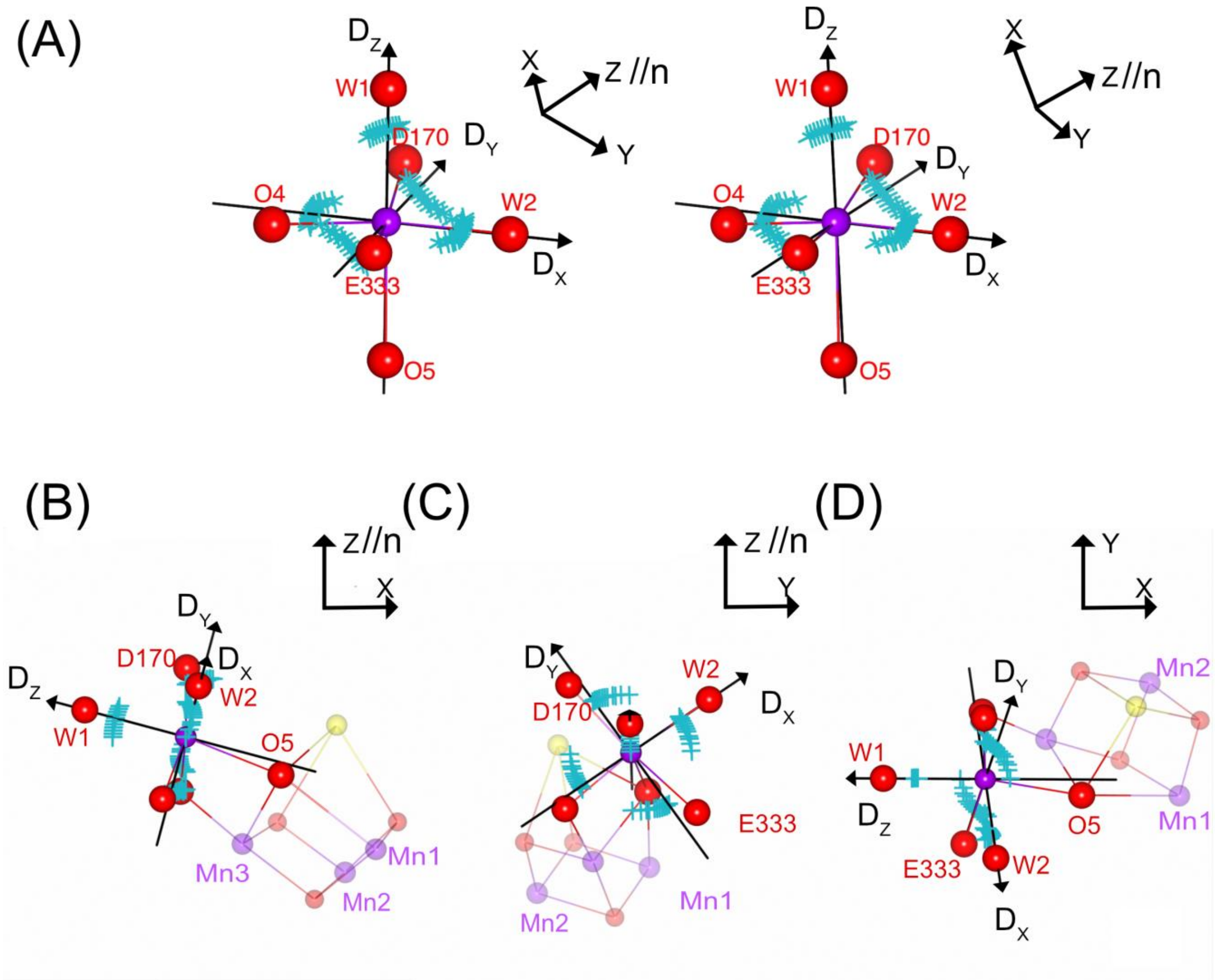

Figure S4. The possible orientations of the $D_X/D_Y/D_Z$ axes relative to the Mn4 in the crystal structures. The Mn4 is located on the origin of the coordinates. The Z-axis is parallel to membrane normal ***n***. The XY-plane is parallel to membrane plane. D_X and D_Z axes are set to the closest direction to Mn4-O(W2) and Mn4-O(W1), respectively. Panel A is stereographic figure, projected to the arbitrary plane. Panels B-D are the projected figures to (B) XZ-, (C) YZ- and (D) XY-planes, respectively. The possible angles for EPR shifts of 70-80 G in the oriented membranes are indicated with the blue cross marks, corresponded to the open circles in fig.3. The red, yellow and purple balls represent O, Ca and Mn, respectively.

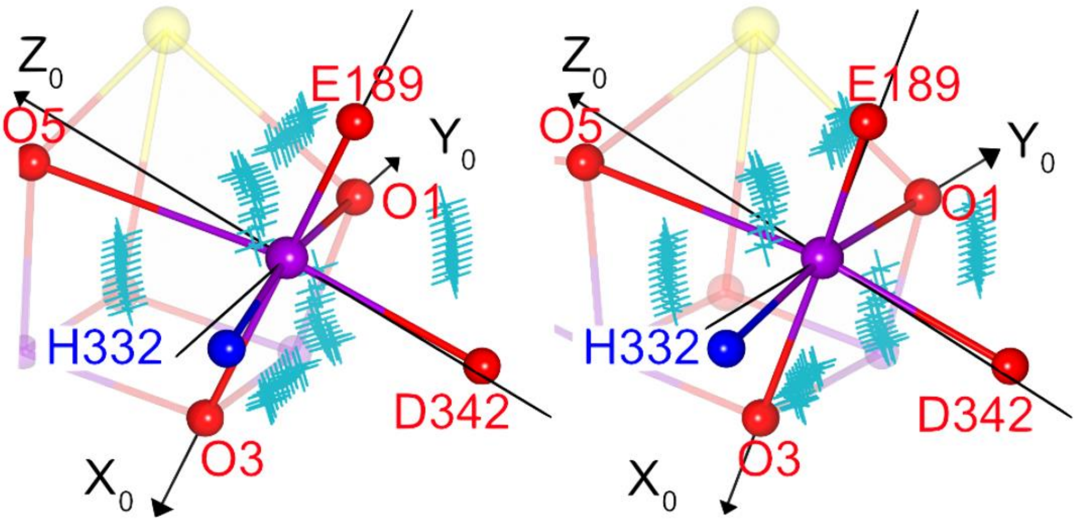

Figure S5. Stereo views of the orientations of the $X_0/Y_0/Z_0$ axes relative to the ligand fields on Mn1. The Mn1 is located on the origin of the coordinates. The axes are set close to Mn1-O3, Mn1-O1 and Mn1-O5, respectively. The possible angles for EPR shifts of 70-80 G in the oriented membranes are indicated with the blue cross marks, corresponded to the open circles in fig.3. The red, yellow and purple balls represent O, Ca and Mn, respectively.

Four-spin model

For the four coupled manganese model, Hamiltonian is written as followings:

$$\mathcal{H} = \sum_{i=1}^{4} g_i \beta \boldsymbol{S_i} \boldsymbol{B_0} + \sum \boldsymbol{I_i} \cdot \boldsymbol{A_i} \cdot \boldsymbol{S_i} + \sum_{i=1}^{4} \boldsymbol{S_i} \cdot \boldsymbol{D_i} \cdot \boldsymbol{S_i} - \sum_{i<j} 2J_{ij} \boldsymbol{S_i} \cdot \boldsymbol{S_j} \quad \text{(5a)}$$

$$\boldsymbol{S_{total}} = \sum_{i=1}^{4} \boldsymbol{S_i} \quad (5b)$$

, where $\boldsymbol{S_i}$ and $\boldsymbol{I_i}$ are the operators of electron spin and nuclear spin of the i-th Mn ion, respectively, g_i is the g-factor, and $\boldsymbol{A_i}$ is the effective hyperfine tensor of the i-th ion, $\boldsymbol{D}_i$ is the tensor of zero-field splittings. J_{ij} is the exchange interaction between the i-th and j-th ions. Total spin $\boldsymbol{S}_{total}$ =13/2 for 1Mn(III)3Mn(IV). For two-spin model, the coupling J_{eff} was assumed between $\boldsymbol{S}$ = 9/2 (cubane frame) and $\boldsymbol{S}$ = 2 (Mn(III)). For four-spin model, the spectral simulations were performed by the diagonalization of the 320×320 matrix for spin Hamiltonian using basic set of wavefunctions $(((\boldsymbol{S}_1 \otimes \boldsymbol{S}_2) \otimes \boldsymbol{S}_3) \otimes \boldsymbol{S}_4)$. In the simulations, Mn1-3 were assumed to be Mn(IV) ($\boldsymbol{S}$ = 3/2), and Mn4 was assumed to be Mn(III) ($\boldsymbol{S}$ = 2). The zero-field splitting term was replaced as followings[1]:

$$d_4 \left[\boldsymbol{S}_{\boldsymbol{4,z}}^2 - \frac{1}{3} S_4(S_4+1)\right] + e_4(\boldsymbol{S}_{\boldsymbol{4,x}}^2 - \boldsymbol{S}_{\boldsymbol{4,y}}^2). \quad \text{(5c)}$$

, where d_4 and e_4 are onsite zero-field splitting parameters for Mn4. For the weak coupling (QM/MM) model, the set of J couplings is following: J_{12}: 30.5 cm^{-1}, J_{13}: 13.0 cm^{-1}, J_{14}: 0 cm^{-1}, J_{23}: 35.5 cm^{-1}, J_{24}: 0 cm^{-1}, J_{34}: -7.6 cm^{-1} [2]. For the strong coupling models, the set of J couplings is following: J_{12}: 200 cm^{-1}, J_{13}: 0 or 200 cm^{-1}, J_{14}: 0 cm^{-1}; J_{23}: 200 cm^{-1}; J_{24}: 0 cm^{-1}. If J_{14} is non-zero, the result is almost the same because the cubane frame is under the strong ferromagnetic couplings. Figure S6 shows the comparison of (a) the QM/MM (weak coupling) model, (b, c) two-spin model and (d-g) the strong coupling models. In (a) the QM/MM model, the low field signal was assigned to the high spin state as g = 6 and g = 10, and the high field signal was upshifted from the g = 4 by mixing of the weakly excited state. In order to simulate the spectrum of the g = 4 signal for the strong coupling models, larger $|J_{34}|$, estimated as > ~30 cm^{-1}, is required. The g = 4 signal was well reproduced using the onsite zero-field splitting d_4 = -3 to -2 with the strong J_{34} coupling.

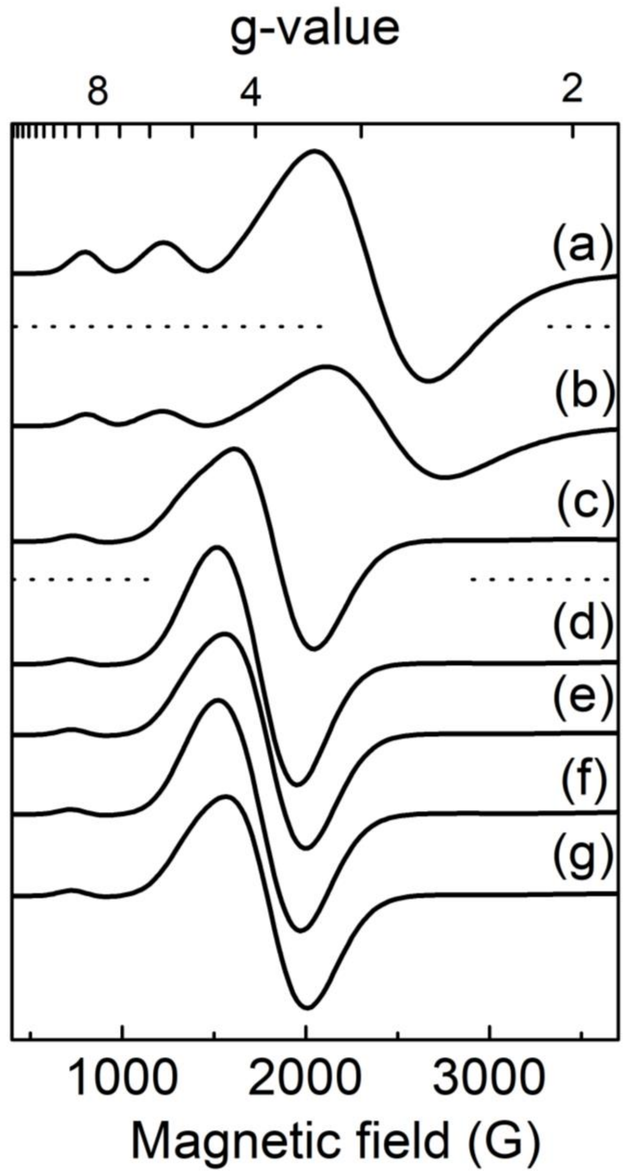

Figure S6. The EPR simulations using (a) the weak coupling model (QM/MM), (b, c) two-spin model and (d-g) the strong coupling models. The exchange couplings in four-spin models [J_{12}, J_{13}, J_{14}, J_{23}, J_{24}, J_{34}] : (a) [30.5, 13, 0, 35.5, 0, -7.6], (d) [200 ,200, 0, 200 , 0, -200], (e) [200 , 0, 0, 200, 0, -50], (f) [200 , 0, 0, 200, 0, -200], (g) [200 ,0, 0, 200, 0, -50]. The exchange couplings J_{eff} in two-spin model: (b) J_{eff} = -2.3 cm^{-1}, (c) J_{eff} = -10 cm^{-1}. (a-c) $d4$ = -3 cm^{-1}, (d-g) $d4$ = -2.3 cm^{-1}, $e4/d4$ = 0.25. Microwave frequency 9.67 GHz; Gaussian linewidth, 350 G.

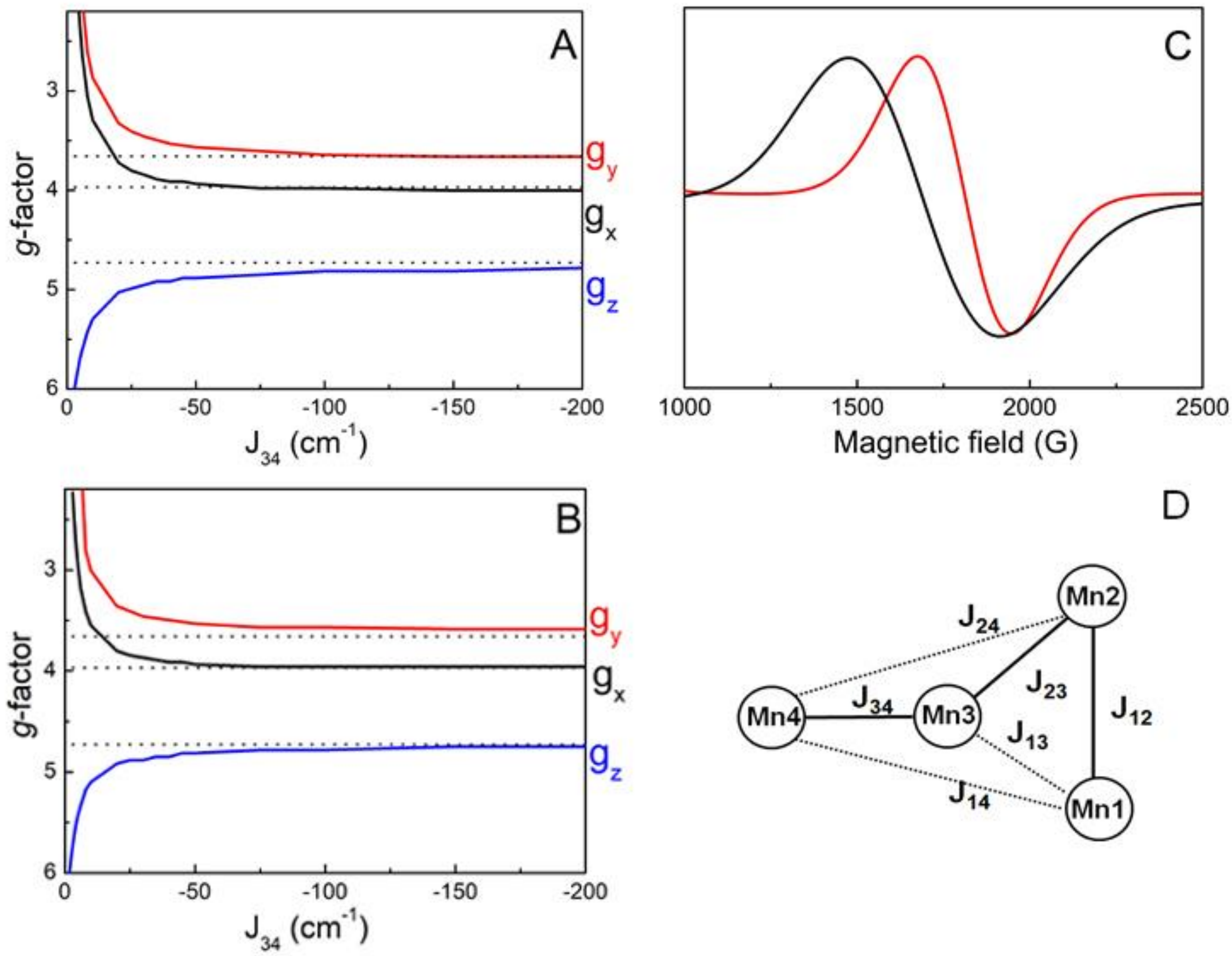

Figure S7. (A, B) J dependence of the resonant conditions for the strongly coupled four-spin model. The parameters: J_{12}: 200 cm^{-1}, J_{13}: 0 cm^{-1}, J_{14}: 0 cm^{-1}, J_{23}: 200 cm^{-1}, J_{24}: 0 cm^{-1}. (A): $d4$, -2 cm^{-1}; $e4/d4$ = 0.25. (B): $d4$, -3 cm^{-1}; $e4/d4$ = 0.25. The solid lines show the resonant fields along each axis. The dotted lines show the resonant condition in the case of the single-spin model for $\boldsymbol{S}$ = 5/2 (Figure S3). (C) The simulated spectra for the oriented sample at (red) 0° and (black) 90° using the parameters of $d4$ = -2.3 cm^{-1}, $e4/d4$ = 0.25 and J_{34} = -50 cm^{-1}. The other conditions are the same as the simulated spectrum in the single-spin model. (D) The scheme for the set of the exchange couplings for the four-spin model. Microwave frequency, 9.67 GHz.

Haddy et al. observed the g = 3.14 and 4.6 signals in Q-band EPR [3]. The g = 3.14 signal was assigned to the ±3/2 transition along the x-axis for $\boldsymbol{S}$ = 5/2. The g = 4.6 signal was tentatively assigned to another transitions within $\boldsymbol{S}$ = 5/2[3]. The Q-band spectrum was well reproduced using the onsite zero-field splitting d4 = -2.3 cm^{-1} in the strong coupling model (Figure S8).

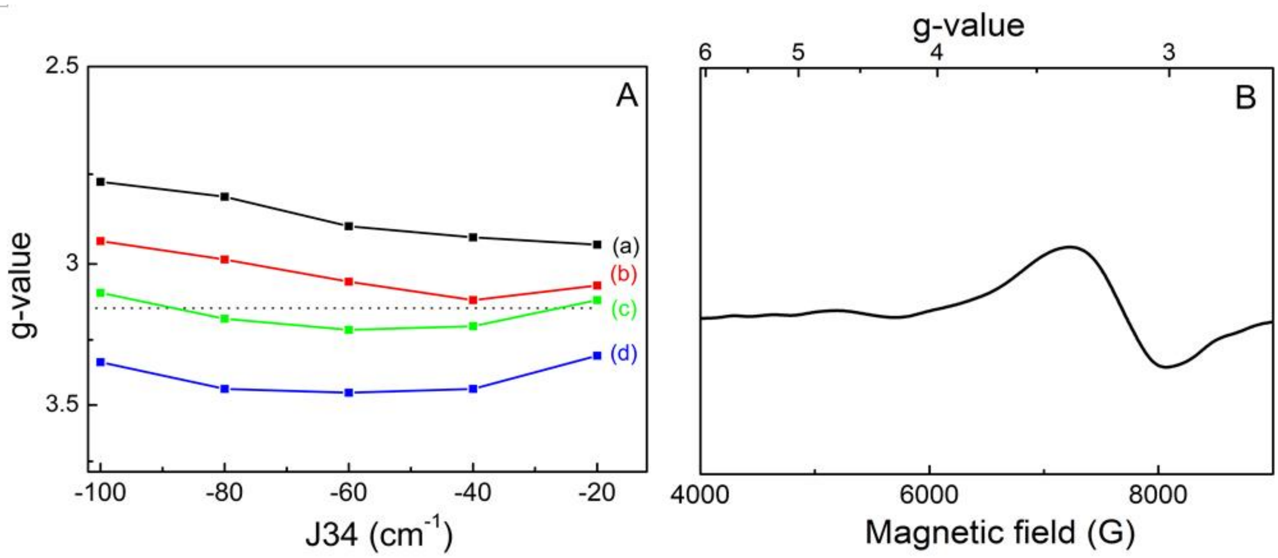

Figure S8. (A) The simulated J dependence of the resonant fields in the strong coupled model at Q-band (34 GHz). The parameter set was used as: J_{12}: 200 cm^{-1}, J_{13}: 0 cm^{-1}, J_{14}: 0 cm^{-1}, J_{23}: 200 cm^{-1}, J_{24}: 0 cm^{-1}, and $e4/d4$ = 0.25; (a) $d4$, -2.0 cm^{-1}; (b) $d4$, -2.2 cm^{-1}; (c) $d4$, -2.4 cm^{-1}; (d) $d4$, -3 cm^{-1}. The dotted line indicates g = 3.14 [3]. (B) The simulated EPR spectrum using d_4 = -2.3 cm^{-1}. The parameters are the same as (A) except for J_{34} = -50 cm^{-1}.

References

(1) Cox, N.; Ames, W.; Epel, B.; Kulik, L. V.; Rapatskiy, L.; Neese, F.; Messinger, J.; Wieghardt, K.; Lubitz, W. Electronic Structure of a Weakly Antiferromagnetically Coupled $Mn^{II}Mn^{III}$ Model Relevant to Manganese Proteins: A Combined EPR, ^{55}Mn-ENDOR, and DFT Study. *Inorg. Chem.* **2011,** *50*, 8238-8251.

(2) Pantazis, D. A.; Ames, W.; Cox, N.; Lubitz, W.; Neese, F. Two interconvertible structures that explain the spectroscopic properties of the oxygen-evolving complex of photosystem II in the S_2 state. *Angew. Chem., Int. Ed.* **2012,** *51*, 9935-9940.

(3) Haddy, A.; Lakshmi, K. V.; Brudvig, G. W.; Frank, H. A. Q-band EPR of the S_2 state of Photosystem II confirms an S=5/2 origin of the X-band *g*=4.1 signal. *Biophys. J.* **2004,** *87*, 2885-2896.